EDGE TURBULENCE SPECTRUM ALTERATIONS DRIVEN BY RESONANT FIELDS

M.V.A.P. HELLER, R.M. CASTRO, Z.A. BRASÍLIO, I.L. CALDAS,
R.P. DA SILVA, TBR-1 TEAM
Institute of Physics,
University of São Paulo,
São Paulo, Brazil

ABSTRACT. An ergodic magnetic structure is generated in the TBR-1 tokamak boundary to handle heat flux and minimize impurity generation. In this work, the effect of this structure on the plasma edge turbulence is investigated. Thus, spectral alterations driven by perturbing magnetic fields created by resonant helical windings are observed in the small tokamak TBR-1. The investigated oscillations are detected with an array of Langmuir and magnetic probes. Spectral and bispectral analyses revealed significant changes induced by the resonant helical windings, mainly in the MHD frequency band. Thus, whereas the known Mirnov oscillation amplitude reduction is observed, the density and potential oscillation spectra are slightly affected. However, the bispectral analysis shows a clear reduction of the wave-wave mode coupling in the MHD frequency range, while the high frequency turbulent coupling is spreadly reduced.

1. INTRODUCTION

Control of the plasma-wall interactions is very important for controlled magnetic fusion research in tokamaks [1-3]. To improve confinement, these machines must have, in the edge, a cold and dense plasma layer to reduce impurities liberation, to avoid the migration of non-ionized impurities to the centre of the column and to have a uniform heat deposition on the vessel and on the limiter. One possible way to attain these objectives is to control plasma edge transport at the edge by the ergodization of magnetic surfaces in the boundary layer. This process can be obtained with resonant helical fields that, when superposed with equilibrium fields, provoke overlapping of magnetic islands and field line ergodization.

Intense fluctuations in the plasma parameters, such as density and potential, are always present in magnetically confined plasmas [1, 2]. Experiments show that anomalous edge particle transport is induced by that electrostatic turbulence [4]. Nowadays, the intensive investigation of edge turbulence and transport is motivated by the unexpected results obtained on large tokamaks [4]. Thus, a better understanding of turbulence and confinement control should be developed for the safe projection of next step devices.

The influence of perturbed magnetic surfaces on plasma edge turbulence has been increasingly investigated theoretically [4-7] as well as experimentally [8-13]. Both natural and externally applied magnetic perturbations produce magnetic islands that can enhance particle transport [8] or create stochastic fields that may degrade confinement [14]. They can also modulate electrostatic turbulence [11], changing some relevant plasma edge characteristics associated with these oscillations, such as the shear layer radial position. Furthermore, these perturbations can reduce the plasma edge turbulence [13] or even stabilize the tokamak discharges [12].

Since the electrostatic turbulence is responsible for the edge anomalous particle transport [3], externally applied magnetic perturbations might be used to control this turbulence and indirectly the electrostatic driven particle transport at the plasma edge. However, until now, in spite of the use of special devices, such as ergodic magnetic limiters (EML) [15] or resonant helical windings (RHW) [16], to produce resonances in this region, this effect has not yet been observed.

Experiments in the TBR-1 tokamak employing external resonant field perturbations, created by RHW, have been performed to control Mirnov oscillations [17], disruptions [18], plasma edge profiles [19] and turbulence [20]. These external coils create both magnetic islands and stochastic field regions through island overlapping [21]. In this work a possible influence of the resonances created by the $m = 4/n = 1$ RHW on the plasma edge turbulence, and on the particle transport induced by this turbulence, has been examined. In this machine, a partial superposition between the magnetic and electrostatic spectra, at the MHD frequency range [22], creates favourable conditions to observe this effect.

For this investigation, a composite system of probes was projected and installed in TBR-1 [22]. A distinguishing feature of these probes is the ability to measure, simultaneously and within a short distance, electrostatic and magnetic fluctuations, and relevant plasma parameters, such as density, potential and temperature.

The data were digitized and submitted to a power spectral analysis to quantify several statistical properties of the observed fluctuations, and to estimate the turbulence driven radial particle flux at the plasma edge [23, 24]. Furthermore, with this spectral analysis, bispectra and bicoherence spectra [23, 24] were computed to verify non-linear wave–wave coupling in these oscillations.

2. EXPERIMENTAL SET-UP

TBR-1 is a small ohmically heated tokamak with a poloidal limiter [25] (Fig. 1(a)). Its main parameters are: major radius $R = 0.30$ m, limiter radius $a = 0.08$ m and vessel radius $b = 0.11$ m. For this experiment, the machine was operated with a central electron temperature $T_e(0) = 1 \times 10^2$ eV, central density $n(0) = 3 \times 10^{18}$ m^{-3}, plasma current $I_p = 8.5$ kA, toroidal field $B_\phi = 0.4$ T and loop voltage $V_\ell < 1.5$ V.

The probe assembly is mounted on a porthole at the top of the tokamak, along the plasma centreline at 45° from the limiter and on a structure that permits a radial movement of the probe in the vessel (Fig. 1(a)). The Langmuir probe array has four wire tips configured in a 2×2 square matrix with a 2×10^{-3} m spacing. Two of the probe tips are connected to measure floating potential fluctuations, $\tilde{\varphi}$, and the other two connected to collect the ion saturation current to measure density fluctuations, $\tilde{n}$. Three other tips of the same dimensions are biased as a triple probe [26] and are used to measure the mean plasma density, n, electron temperature, T_e, and floating potential. There are also four coils, to measure magnetic field component fluctuations, two poloidally and two radially oriented, mounted in the same system at 2.3×10^{-2} m from the Langmuir probes, Fig. 1(b).

The probe signals are digitally recorded at a sampling frequency of 1 MHz to allow measurements up to the Nyquist frequency of 500 kHz. All measured quantities are taken in the time interval of 2 ms during the current flat-top and averaged over four consecutive shots. The analysed data consist of 62 samples of 128 points. In the present analysis, the effect of temperature fluctuations is neglected in the computation of density fluctuations in terms of saturation current fluctuations, and in the computation of the fluctuating plasma potential from the measured floating potential fluctuations.

The external magnetic field perturbation is created by electric currents circulating in a set of helical windings located externally around the torus [1, 16]. There are four pairs of these windings [17] with helicity determined by the following approximated winding law: $4\theta - \phi = ct$, where θ and ϕ are the poloidal and toroidal angles, respectively. Therefore, these coils produce a perturbation field with dominant helicity $m/n = 4/1$ and average poloidal field amplitude $b_r/B_\phi \leq 1\%$ at the limiter radius [21]. The currents circulating in those coils were adjusted in $I_h = 180$ A, and they were switched on after the plasma current had reached steady values.

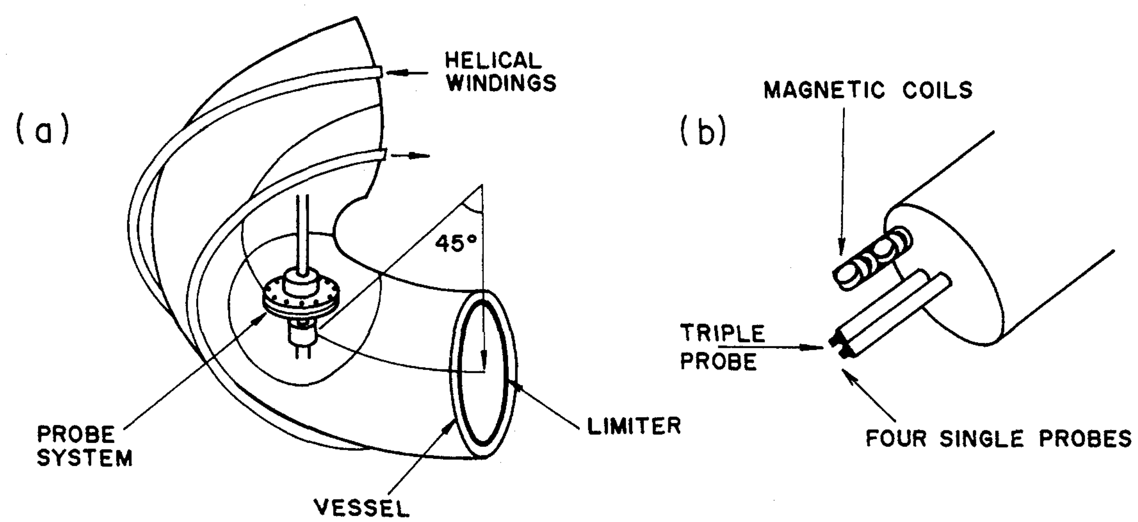

FIG. 1. (a) Section of the tokamak illustrating measurement position. (b) Probe system viewing head.

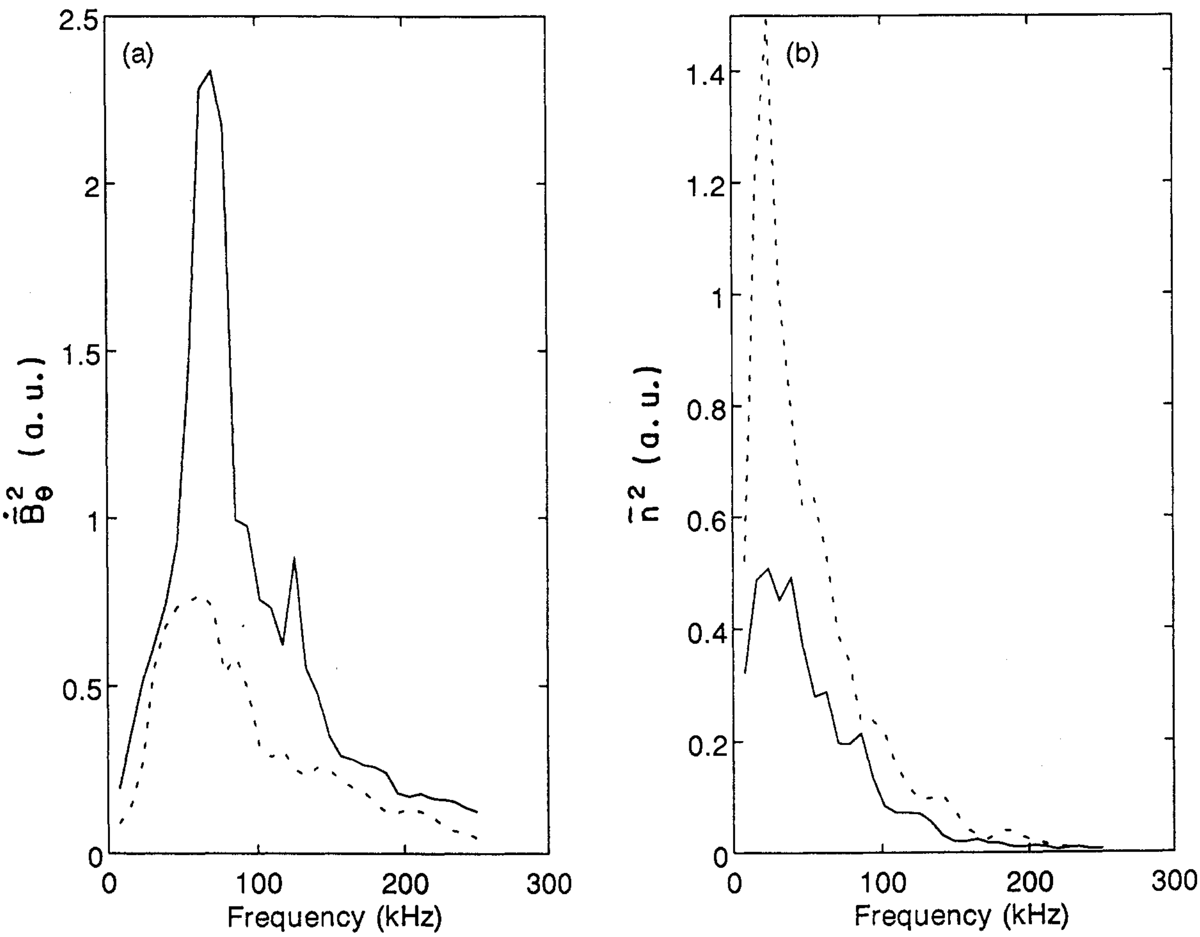

FIG. 2. (a) Power spectra of magnetic poloidal fluctuations with RHW (dashed curve) and without RHW (full curve) for r/a = 1.16. (b) Power spectra of density fluctuations with RHW (dashed curve) and without RHW (full curve) for r/a = 0.87.

3. SPECTRUM CHANGES

As can be seen in Fig. 2, the electrostatic and magnetic fluctuation power is basically localized below 150 kHz. Unlike most present tokamak plasmas, in TBR-1 the main electrostatic frequencies are smaller than the Mirnov frequencies. This distinctive peculiarity is a consequence of the plasma radius and the magnetic toroidal field values and fits known scaling laws [1, 2]. Furthermore, there is an unusual partial superposition of the frequency power spectra of these two oscillations. These characteristics create favourable conditions to investigate any possible correlation or non-linear coupling between these two spectra.

The fluctuating density and magnetic spectra shown in Fig. 2 were computed from data measured at the radial positions $r/a = 0.87$ and $r/a = 1.16$, respectively. As previously reported, the RHW reduce the Mirnov oscillation amplitudes [14, 16] and slow down their frequencies [17, 20] (Fig. 2(a)). Although the helical current increases the density fluctuations (Fig. 2(b)) at this radial position, this effect is not so evident in the other positions nearer the edge. A similar alteration was induced (in the outer part of the inversion shear layer) by an ergodic divertor in the Tore Supra tokamak [13].

Figure 3 shows the magnetic field geometry corresponding to the spectra shown in Fig. 2(a). These Poincaré maps were computed, for those discharges with an $m = 2/n = 1$ MHD dominant mode, with (Fig. 3(a)) and without (Fig. 3(b)) the resonant perturbations created by the $m = 4/n = 1$ helical windings. While, in the unperturbed map (Fig. 3(b)), $m/n = 2/1$, 3/1 and other smaller islands can be recognized, the applied field destroys the magnetic surfaces in an ergodic layer of about 1×10^{-2} m radial width at the edge (Fig. 3(a)). This ergodic region is centred around a safety factor value of $q = 4$ and does not include the $q = 2$ islands. In this case the stochasticity parameter [21], computed for the

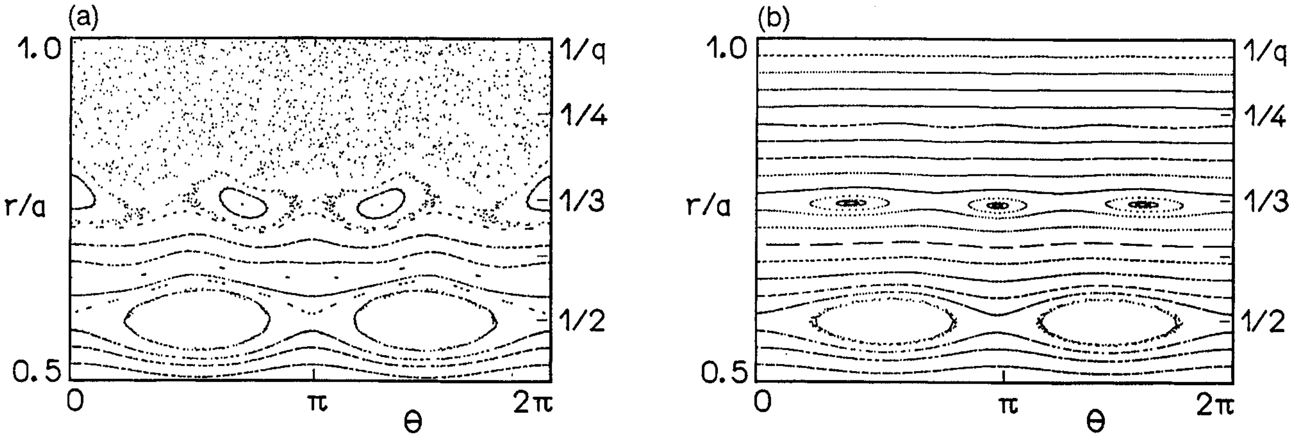

FIG. 3. Poincaré maps showing the poloidal magnetic field line configurations (a) with RHW and (b) without RHW.

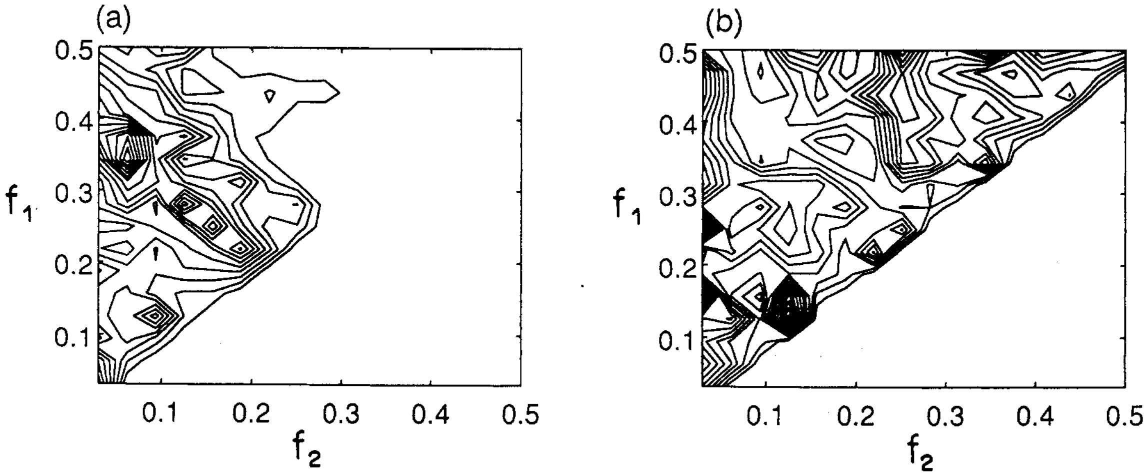

FIG. 4. (a) Auto-bicoherence contour of magnetic poloidal fluctuations, with RHW, r/a *= 1.16. (b) The same without RHW (frequency normalized to Nyquist frequency, data filtered at 250 kHz).*

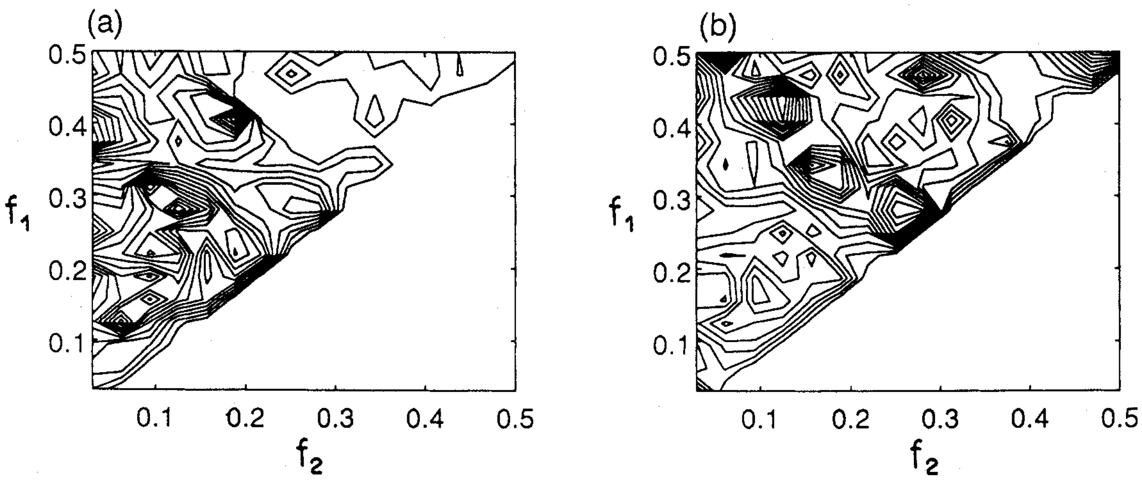

FIG. 5. (a) Auto-bicoherence contour of density fluctuations with RHW, r/a *= 0.87. (b) The same without RHW (frequency normalized to Nyquist frequency, data filtered at 250 kHz).*

$m = 3/1$ and $m = 4/1$ island superpositions, was $s \cong 1$. Thus, in this experiment, the RHW created a field line configuration similar to those obtained in the tokamaks TEXT [9] and Tore Supra [3] with ergodic divertors (although these divertor configurations, with higher m, create thinner ergodic layers more appropriate to plasma confinement).

The bispectra analysed in this work clearly reveal changes produced by the RHW as shown in the next figures. To investigate changes caused by the RHW in the wave-wave coupling, auto-bispectra and auto-bicoherence have been computed for $\tilde{n}$ and $\dot{\tilde{B}}_\theta$ time series. Thus, Figs 4 and 5 show the squared bicoherence contour plots, computed from the same data used in Fig. 2. This squared auto-bicoherence, from a single spatial point measurement, is defined as [23]:

$$b^2(f_1, f_2) = \frac{|\langle X(f_1)X(f_2)X^*(f_1 + f_2)\rangle|^2}{\langle |X(f_1 + f_2)|\rangle^2 \langle |X(f_1)X(f_2)|\rangle^2} \tag{1}$$

with $\langle \ldots \rangle$ denoting the ensemble average, $X(f)$ the fast Fourier transform of the analysed fluctuating quantity $x(t)$, and * denotes complex conjugate. This function describes the coupling between a triplet of modes at frequencies f_1, f_2 and $f = f_1 \pm f_2$. When the modes of a considered triplet vary independently as in the random noise, $b^2 = 0$, and when these modes are quadratically coherent, $b^2 = 1$. Thus, the bicoherence spectrum measures the fraction of power due to the quadratic interaction. As usual, owing to symmetry relations, the b^2 values are only plotted within the triangle $0 \le f_2 \le f_N/2$ and $f_2 \le f_1 \le f_N - f_2$, where f_N is the Nyquist frequency.

Although no prominent peaks can be identified in Figs 4 and 5, a low level of non-linear coherent interactions much larger than the statistical uncertainty $1/M = 0.02$ ($M = 62$ is the number of realizations) can be identified. This is significant mainly for the low frequency modes which present the highest bispectral amplitudes. However, even so, this bispectral analysis clearly indicates a considerable level of non-coherent strong turbulence interactions. With the reduction of the Mirnov oscillation amplitudes (Fig. 2(a)), the non-linear couplings shown in Figs 4 and 5 are reduced and, consequently, the interaction becomes less coherent.

Figure 6 shows the cross-bicoherences computed with the Fourier amplitudes $\tilde{n}(f)$ and $\dot{\tilde{B}}_\theta(f)$, corresponding to the power spectra of Fig. 2, from data obtained at $r/a = 0.87$ and 1.16. These cross-bicoherences, from two spatial-point measurements, have the same qualitative characteristics as the previous one, but with higher values for discharges without the resonant perturbations.

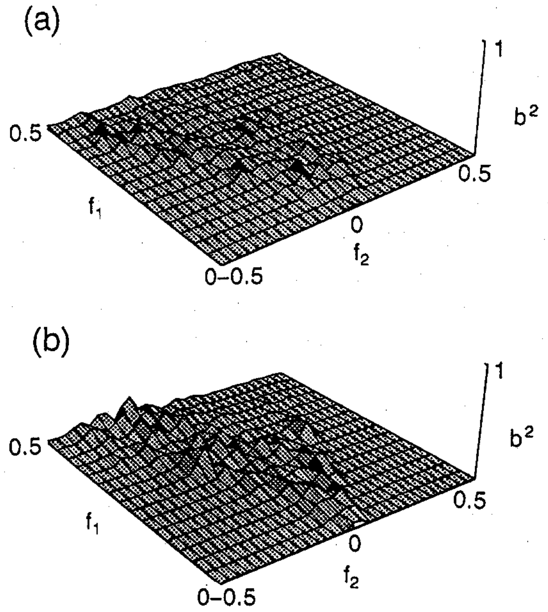

FIG. 6. (a) Cross-bicoherence between magnetic poloidal fluctuations and density fluctuations, with RHW. (b) The same without RHW (frequency normalized to Nyquist frequency, data filtered at 250 kHz).

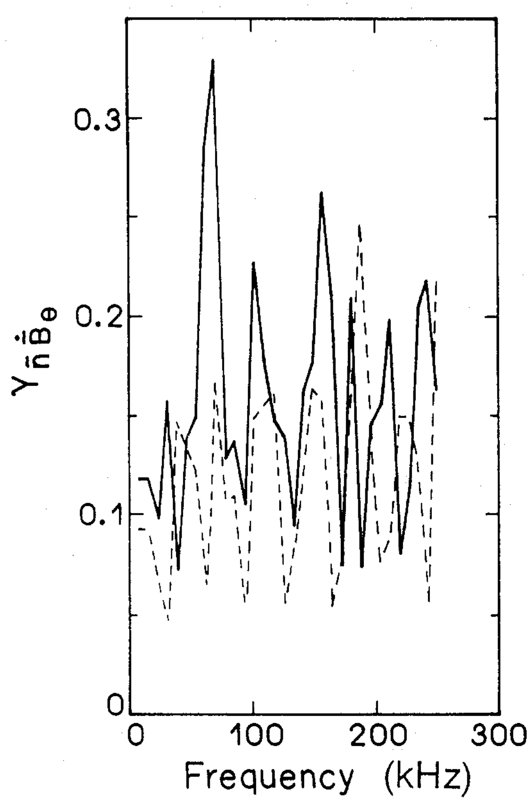

FIG. 7. Coherence spectra of density and magnetic poloidal fluctuations, with RHW (dashed curve) and without RHW (full curve) at r/a = 0.87.

Figure 6(a) shows that non-linear coupling is more intense between f_1 and $f_1 - f_2$ in the low frequency band. The amplitude reduction caused by the perturbation is also more distinct. These conclusions suggest that a high magnetic activity might alter the Gaussian probability distribution functions, creating coherent structures not yet clearly observed on the tokamak electrostatic turbulence [27–29], or the intermittency recently reported [30]. However, as can be seen in Fig. 7, the levels of linear coherence between $\tilde{n}$ and $\tilde{\dot{B}}_\theta$ are low, and their values are not much affected by the magnetic perturbation. Nevertheless, peaks in the MHD frequency band (such as those shown in Fig. 7) are attenuated by this perturbation.

An estimation of the radial particle flux spectrum due to electrostatic fluctuations can be made from the correlation of measured density and potential fluctuations [23, 24]

$$\Gamma(f) = \frac{1}{B_\phi} |\tilde{n}|^{1/2} |\tilde{\varphi}|^{1/2} k_\theta(f) \gamma_{\tilde{n}\tilde{\varphi}} \sin\theta_{\tilde{n}\tilde{\varphi}} \qquad (2)$$

where $k_\theta(f)$ is the wavenumber obtained from a pair of floating Langmuir probes poloidally separated; $\theta_{\tilde{n}\tilde{\varphi}}$ and $\gamma_{\tilde{n}\tilde{\varphi}}$ are, respectively, the phase angle and the coherence between $\tilde{n}$ and $\tilde{\varphi}$. Figure 8 shows that this transport spectrum is also modified by the resonant perturbation, though the integrated transport is only slightly affected.

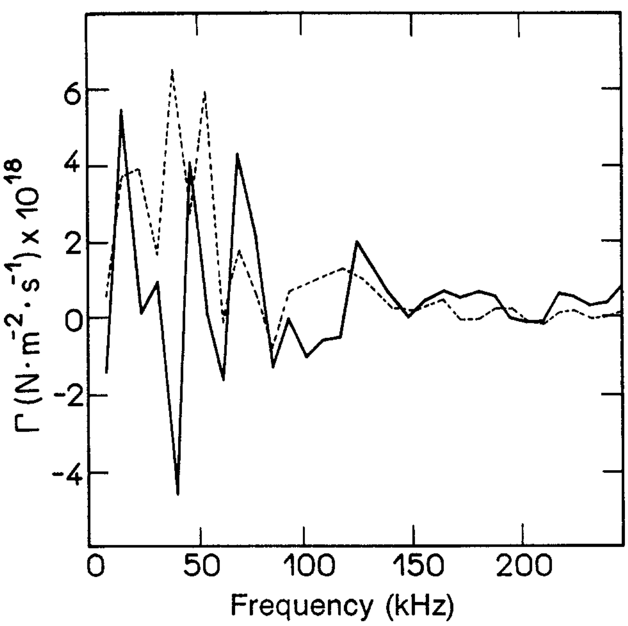

FIG. 8. Particle flux spectra with RHW (dashed curve) and without RHW (full curve), at r/a = 0.87.

4. CHANGES IN THE FLUCTUATION RADIAL PROFILES

In this section the effect of externally created resonances on the radial profiles of some turbulence parameters is presented.

Digital spectral analysis is used to compute the wavenumber–frequency spectrum $S(k,f)$, reducing the

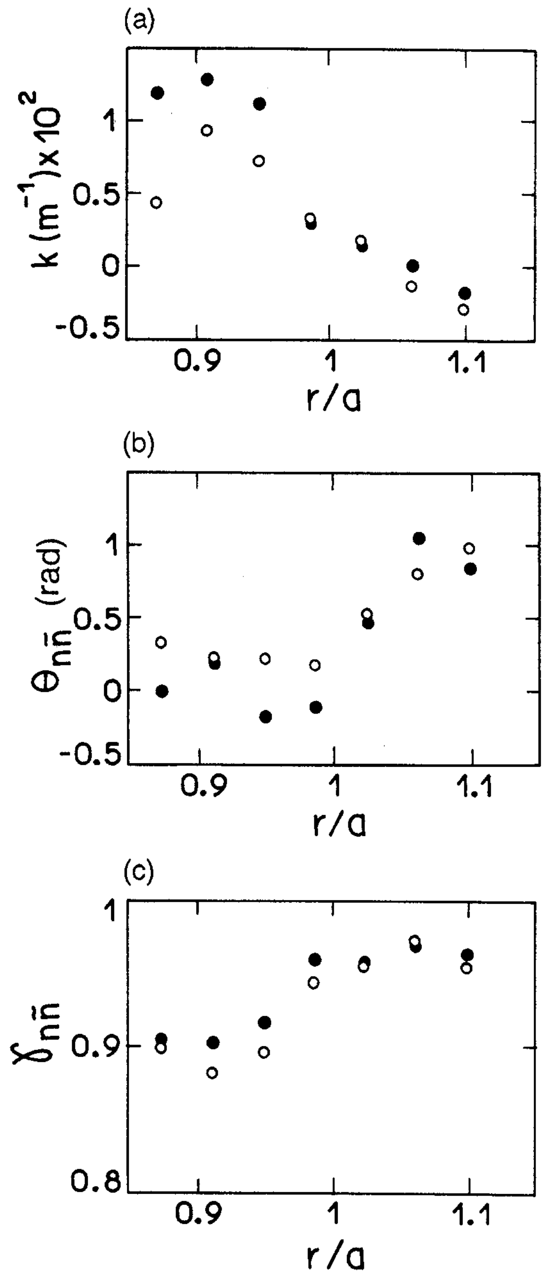

FIG. 9. (a) The k profile for density fluctuations, (b) phase angle profile for density fluctuations and (c) coherence profile for density fluctuations, with RHW (open circles) and without RHW (closed circles).

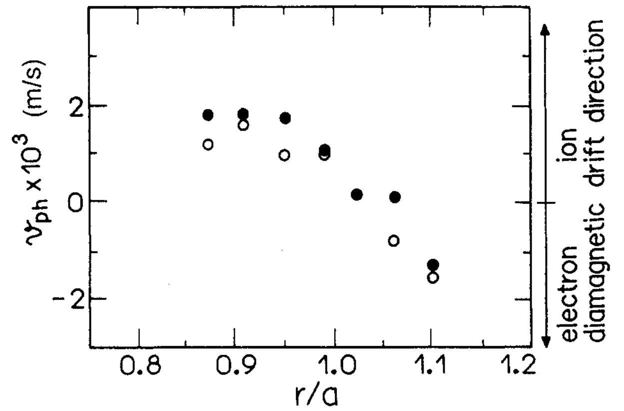

FIG. 10. Phase velocity profile for density fluctuations with RHW (open circles) and without RHW (closed cirlces).

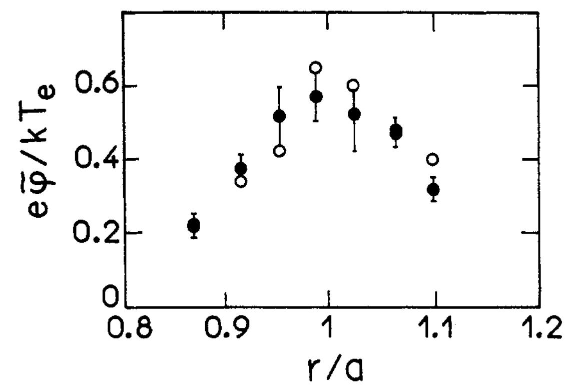

FIG. 11. The $e\bar{\varphi}/kT_e$ profile with RHW (open circles) and without RHW (closed circles).

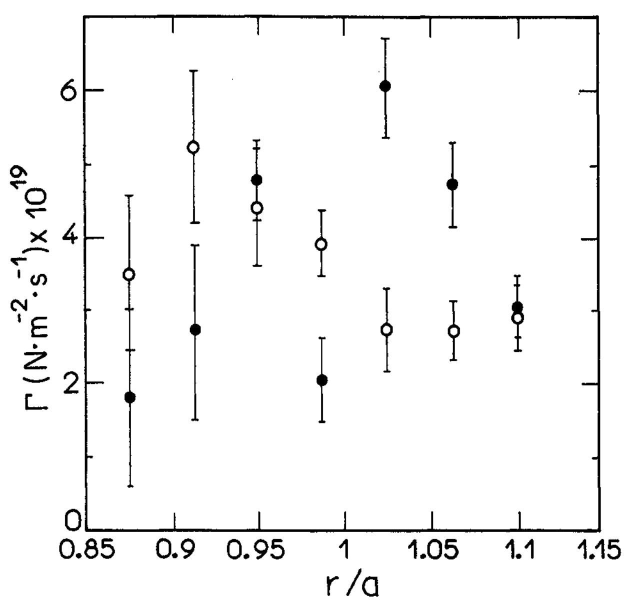

FIG. 12. Particle flux profile with RHW (open circles) and without RHW (closed circles).

information contained in the times series of $\tilde{n}(t)$ or $\tilde{\varphi}(t)$ obtained from two poloidally separated probes. Using $S(k,f)$, a statistical dispersion relation, $k(f)$, the coherency spectrum, $\gamma(f)$, and the phase velocity, v_p, can be calculated for both $\tilde{n}$ and $\tilde{\varphi}$. The phase difference between these two oscillations, $\theta(f)$, can also be computed. From these frequency distributions, average values were obtained for different radial positions, as shown in Fig. 9.

Inside the plasma, the average wave vector $\bar{k}$ is reduced by the RHW, whereas their values outside the limiter are not altered (Fig. 9(a)). The coherency γ profile (Fig. 9(b)) is only slightly modified, but the θ profile is altered (Fig. 9(c)), affecting the transport values.

Inside the plasma, in the region accessible to the probes, the poloidal phase velocity has the same order of magnitude and the same direction as the ion diamagnetic drift velocity. Furthermore, no reversal in the directions of phase velocity and electrical field is observed inside the plasma (Fig. 10). Thus, there is no evidence of the existence of a shear layer [22], as has been observed in other tokamaks [4]. In the TEXT tokamak a displacement of the shear layer to the outside was observed, as the Mirnov oscillation amplitudes decreased [11]. In TBR-1 the absence of a shear layer in the plasma remains even with the RHW perturbation that reduces those oscillations. This result does not contradict the observation in TEXT, but rather confirms previous indications that in TBR-1 no shear layer is observed near the limiter. However, the existence or not of a shear layer in the innermost position accessible to the probes cannot be determined. This absence of a shear layer might be due to the lack of a peak in the plasma potential radial profile caused by the plasma edge electron loss, typical of a small tokamak [25]. The non-observation of a shear layer was also reported in the Tokapole II, another small tokamak operating in low density regimes [31].

Figure 11 shows the radial profile of the normalized floating potential. No appreciable alteration is produced by the RHW, although it affects the power frequency spectra in this region. The same conclusions are valid for the integrated values of the turbulence induced transport whose radial profile is shown in Fig. 12.

5. CONCLUSIONS

In the last few years, several characteristics of plasma edge turbulence have been measured, but no complete theory has been proposed yet to explain the main observations. Thus, the plasma edge turbulence in TBR-1, as well as in other tokamaks, cannot be successfully described as a result of drift waves because the fluctuations considered do not satisfy the Boltzmann relation [4, 22]. On the other hand, the computed product $k_\theta \rho_i$ is too high to be described by the present rippling mode theories [4, 22].

In this context, the influence of the resonant magnetic fields on the turbulence has been investigated theoretically [5] and experimentally [7, 8, 11], and the present work contributes to determine this influence, investigating the effect of the controlled MHD oscillations on the electrostatic turbulence.

The measured equilibrium profiles do not show any significant radial modification, but, as has been suggested [14, 16, 32], even small radial profile modifications (produced by the used 4/1 RHW) to the resonant magnetic surfaces could be enough to explain the spectra alterations reported in this work.

In this experiment the helical perturbations created an ergodic layer between the $m = 2/n = 1$ islands and the limiter.

The reported experiment and spectral analysis indicate that externally created magnetic resonances affect, in the plasma edge of the tokamak TBR-1, the electrostatic turbulence and the radial particle transport driven by this turbulence. Although the electrostatic turbulence and the anomalous transport are not noticeably reduced, as the Mirnov oscillations are, their spectra are significantly modified by the 4/1 RHW. Thus, inside the plasma, the electrostatic turbulence has its average wave vector reduced. Furthermore, changes induced on the phase difference between $\tilde{n}(f)$ and $\tilde{\varphi}(f)$ alter significantly the radial particle transport $\Gamma(f)$. On the other hand, these spectrum alterations are not so significant in the scrape-off layer as they are inside the plasma.

No shear layer at the plasma edge is identified in this experiment. This contrast with other tokamak experiments suggests the possible presence of a shear layer inside the plasma, in a region not accessible to the diagnostic available in TBR-1. In fact, as observed in TEXT [11], in a high MHD activity regime, such as those considered here, the shear layer position depends on the magnetic fluctuation amplitude. Thus, the turbulence enhancement observed at $r/a = 0.87$, in the discharges with helical currents, should correspond to the enhancement (in the outer part of the inversion shear layer) induced by an ergodic divertor in the Tore Supra tokamak [13].

At the plasma edge the transport is inward at some low frequency ranges, as was observed in the ADITYA tokamak [33]. As this negative flux is reduced by the RHW, the integrated transport increases at this region. On the other hand, no inward flux is observed in the scrape-off layer.

The described alterations on the auto- and cross-bispectra reveal a reduction caused by the RHW on the quadratic non-linear coupling in the broad band turbulence. Thus, this coupling is reduced with the resonant perturbations. This effect is especially significant for the cross-bispectra computed from the fluctuating $\tilde{n}(f)$ and $\dot{\tilde{B}}_\theta(f)$. These changes indicate that the control of the Mirnov oscillations may indirectly modify the electrostatic transport at the plasma edge and influence the plasma–wall interactions.

The results described in this work show the influence of the magnetic oscillations on the electrostatic turbulence. Other examples of this influence can be mentioned, such as the modulation of electrostatic turbulence by a dominant MHD mode [11], and correlations between magnetic turbulence and the electrostatic transport [34, 35]. As suggested in several references [15, 32], this influence may be used to control plasma–wall interactions and to improve plasma confinement.

ACKNOWLEDGEMENTS

The authors acknowledge discussions with Dr. R.D. Bengtson and Dr. S.C. McCool (Fusion Research Center, The University of Texas at Austin), Dr. I.H. Tan (The University of Wisconsin), the referees' suggestions, and the technical support given by Dr. A.N. Fagundes and Mr. W.P. de Sá (IF-USP). The authors also thank Ms. G.Y. Oda, for the computer code used in the construction of the Poincaré maps. This work was partially supported by FAPESP and CNPq.

REFERENCES

[1] TSUI, H.Y.W., et al., J. Nucl. Mater. **196–198** (1992) 794.
[2] ROBINSON, D.C., in Small Scale Turbulence and Anomalous Transport in Magnetized Plasmas (Proc. Int. Workshop, Cargèse, 1986), Éditions de Physique, Cargèse (1986) 21; Plasma Phys. Control. Fusion B **35** (1993) 91.
[3] GROSMAN, A., et al., Plasma Phys. Control. Fusion **32** (1990) 1011.
[4] WOOTTON, A.J., et al., Phys. Fluids B **2** (1990) 2879.
[5] FINN, J., et al., Phys. Fluids B **4** (1992) 1152.
[6] RECHESTER, A.H., STIX, T.H., Phys. Rev. Lett. **36** (1976) 587.
[7] KIM, Y.J., et al., Phys. Fluids B **3** (1991) 674.
[8] McCOOL, S.C., et al., J. Nucl. Mater. **176&177** (1990) 716.
[9] McCOOL, S.C., et al., Nucl. Fusion **30** (1990) 167.
[10] FOSTER, M.S., The Effects of Externally Imposed Magnetic Perturbations on Plasmas in TEXT, Rep. FRCR No. 426, Univ. of Texas, Fusion Res. Center, Austin, TX (1992).

[11] LIN, H., Turbulence and Transport Studies in the Edge Plasma of the TEXT Tokamak, Rep. FRCR No. 401, Univ. of Texas, Fusion Res. Center, Austin, TX (1991).
[12] VALLET, J.C., et al., Phys. Rev. Lett. **67** (1991) 2662.
[13] HESS, W.R., et al., in Controlled Fusion and Plasma Physics (Proc. 20th Eur. Conf. Lisbon, 1993), Vol. 17C, Part III, European Physical Society, Geneva (1993) 1087.
[14] ROBINSON, D.C., Nucl. Fusion **25** (1985) 1101.
[15] KARGER, F., LACKNER, K., Phys. Lett. A **61** (1978) 385.
[16] PULSATOR TEAM, Nucl. Fusion **25** (1985) 1059.
[17] VANNUCCI, A., et al., Nuovo Cim., D **10** (1988) 1193.
[18] ARAÚJO, M.S.T., et al., Investigations of Disruptions with Resonant Helical Windings (in preparation);
VANNUCCI, A., et al., Plasma Phys. Control. Fusion **31** (1989) 147.
[19] RIBEIRO, C., et al., in Controlled Fusion and Plasma Heating (Proc. 17th Eur. Conf. Amsterdam, 1990), Vol. 14B, Part I, European Physical Society, Geneva (1990) 349.
[20] HELLER, M.V.A.P., et al., in Controlled Fusion and Plasma Heating (Proc. 20th Eur. Conf. Lisbon, 1993), Vol. 17C, Part II, European Physical Society, Geneva (1993) 683.
[21] FERNANDES, A.S., et al., Plasma Phys. Control. Fusion **30** (1988) 1203.
[22] CASTRO, R.M., et al., Nuovo Cim., D **15** (1993) 983.
[23] POWERS, E.J., Polyspectral Analysis and Its Applications, Internal Rep., Univ. of Texas, Austin, TX (1990).
[24] RITZ, C.P., et al., Phys. Fluids B **1** (1989) 153.
[25] DA SILVA, R.P., NASCIMENTO, I.C., in Plasma Physics (Proc. Int. Conf. New Delhi, 1989), Vol. 1, Inst. for Plasma Res., Bhat, New Delhi (1989) 93.
[26] CHEN, S.L., SEKIGUCHI, T., J. Appl. Phys. **36** (1965) 2363.
[27] FILIPPAS, A.V., Conditional Statistical Analysis of Plasma Fluctuations in the Edge of TEXT-U Plasma, Rep. FRCR No. 433, Univ. of Texas, Fusion Res. Centre, Austin, TX (1993).
[28] TSUI, H.Y.W., et al., Phys. Fluids B **5** (1993) 1274.
[29] TSUI, H.Y.W., et al., Phys. Rev. Lett. **70** (1993) 2565.
[30] JHA, R., et al., Phys. Rev. Lett. **69** (1993) 1375.
[31] TAN, I.H., PRAGER, S.C., Phys. Rev. Lett. **68** (1992) 1714.
[32] FURTH, H.P., et al., Phys. Fluids **6** (1963) 459.
[33] JHA, R., et al., Nucl. Fusion **33** (1993) 1201.
[34] OHYABU, N., et al., Phys. Rev. Lett. **58** (1987) 120.
[35] MALACARNE, M., et al., Fluctuations During JET Discharges with H-Mode, Rep. JET-P, JET Joint Undertaking, Abingdon, Oxfordshire (1987).

(Manuscript received 24 January 1994
Final manuscript received 3 June 1994)